To be presented in The First International Conference on Advances in Experimental Structural Engineering
AESE 2005, July 19-21, 2005, Nagoya, Japan

COMPRESSIVE BEHAVIOR OF BUCKLING-RESTRAINED BRACE GUSSET CONNECTIONS

MIN-LANG LIN [1], KEH-CHYUAN TSAI [2], PO-CHIEN HSIAO[3] ,and CHENG-YU TSAI[4]

[1] National Center for Research on Earthquake Engineering, Taipei, Taiwan
Email: mllin@ncree.org
[2] National Center for Research on Earthquake Engineering, Taipei, Taiwan
Email: kctsai@ncree.org
[3] Department of Civil Engineering, National Taiwan University, Taipei, Taiwan
Email: r91521221@ntu.edu.tw
[4] Department of Civil Engineering, National Taiwan University, Taipei, Taiwan
Email: r92521203@ntu.edu.tw

ABSTRACT

Buckling-restrained braced frames (BRBF) have gained notable acceptance in Taiwan recently because of its excellent seismic performance and cost-effectiveness. Compare to the traditional concentric braces, buckling-restrained braces (BRBs) have a high compression strength similar to the tension yielding behavior. The gusset connections must be designed to prevent instabilities when transmit high compression forces of the BRBs. In this paper, experimental behavior of a buckled gusset connections in a full-scale 3-story 3-bay CFT/BRB frame specimen tested in the structural laboratory of NCREE is presented, theoretical study and finite element analysis of gusset connections are also described in this paper. In order to investigate the BRBF system subjected to the bi-directional earthquake loads, a full-scale 2-story single-bay BRBF specimen has been constructed for testing in March of 2005. In order to examine the effectiveness of various stiffening schemes for the gusset plate, results of the finite element analysis are presented. It's illustrated from the gusset plate buckling analysis that proper stiffeners are effective to increase the buckling strength of the gusset plate.

INTRODUCTION

Through international collaboration between researchers in Taiwan, Japan, and the United States, a full-scale 3-story 3-bay CFT column with the buckling restrained braced composite frame (CFT/BRBF) specimen was tested in the structural laboratory of National Center for Research on Earthquake Engineering (NCREE) in October 2003. Being the largest and most realistic composite CFT/BRB frame ever tested in a laboratory, the test provides a unique data set to verify both computer simulation models and seismic performance of CFT/BRB frames. In this series of tests, the buckling of the gusset plates were also examined in various stages of the tests. In March 2005, another full-scale 2-story single-bay BRBF specimen is ready for testing in NCREE to investigate the BRBF system and the brace-to-gusset connection details subjected to the bi-directional earthquake loads. The frame is to be tested using the substructure pseudo-dynamic testing procedures incorporating the networked testing techniques developed in NCREE. This paper discusses the buckling responses of the gusset plates in the 3-story CFT/BRBF and the finite element analysis made for the verification of the gusset plate designs in the 2-story BRBF.

EXPERIMENT OF A FULL-SCALE 3-STORY 3-BAY CFT/BRB COMPOSITE FRAME

The 3-story CFT/BRB frame shown in Fig. 1 has been employed in this experimental research. Only the two exterior beam-to-column joints in each floor are moment connections, all other beam-to-column connections are assumed not to transfer any bending moment. The BRBs are installed in the center bay. Square CFT columns are chosen for the two exterior columns while the center two columns are circular CFTs. The material is A572 Gr.50 for all the steel beams and columns, while the compression strength *fc'* of the concrete filled in CFT columns is 35MPa. The displacement-based seismic design (DSD) procedures were adopted and the final selections of structural members are given in Table 1. The supporting beams above the BRBs satisfy the capacity design principal considering the strained hardened BRBs and an unbalanced vertical load resulted from the difference of the peak BRB compressive and tensile strengths. The fundamental vibration period is about 0.68 second. Three different types of moment connections, namely through beam, external diaphragm and bolted end plate types, varying from the first floor to the third floor were fabricated for the exterior beam-to-column connections. Three types of BRBs, including the single-core, double-core (Uang et al. 2004) and the all-metal BRBs, were adopted in the three different floors. In particular, two single-core unbonded braces (UBs), each consisting of a steel flat plate in the core, were donated by Nippon Steel Company and installed in the second floor. Each UB end to gusset connection uses 8 splice plates and 16-24mmϕ F10T bolts. The two BRBs installed in the third story are double-cored constructed using cement motar infilled in two rectangular tubes (Tsai et al.,2002) while the BRBs in the first story are also double-core but fabricated with all-metal detachable features (Tsai and Lin, 2003a). Each end of the double-core BRB is connected to a gusset plate using 6- and 10-24mmϕ F10T bolts at the third and first floor, respectively. No stiffener was installed at the free edges of any gusset before the testing. The experimental program utilizes pseudo dynamic testing (PDT) procedures to simulate the earthquake load effects imposed on the test structure. Based on the results of the pre-test analyses, conducted using PISA3D (Tsai and Lin, 2003b) and OpenSees (http://opensees.berkeley.edu/), two earthquake records were chosen among strong motion records collected during recent earthquakes. The two earthquake records are TCU082-EW (from the 1999 ChiChi earthquake) and LP89g04-NS (from the 1989 Loma Prieta earthquake), both of which are considered to represent general motions without near-field directivity effects. The original test plan was to scale these two records in acceleration amplitude to represent four separate pseudo-dynamic loading events, which were sequenced as follow: (1) TCU082 scaled to represent a 50/50 hazard intensity, i.e., with a 50% chance of exceeding in 50 years, (2) LP89g04 scaled to a 10/50 hazard intensity, which represents the design basis earthquake, (3) TCU082 scaled to a 2/50 hazard, and (4 LP89g04 scaled to a 10/50 hazard – identical to loading (2). Fig.2 shows the actual applications of the ground motions in the PDTs for the CFT/BRB frame specimen.

As noted above, four earthquake ground accelerations scaled to three different PGAs were planned for the PDT of the CFT/BRB frame specimen. However, some unexpected events encountered during the testing. In the Test No. 1, due to the buckling of the gusset plate occurred at the brace to beam connection in the first story, the test stopped at the time step of 12.3 second. Then stiffeners were added at the free edges of all the gusset plates underneath the floor beams. Then test resumed using the same ground accelerations as Test No.1 in reversed direction. In test No.4, the PDT test was stopped at the time step of 12.54 second due to the crack on the top of concrete foundation near the gusset plate for the south BRB-to-column joint were observed. After one pair of angles was installed bracing the stiffener to the two anchoring steel blocks, the test resumed again by applying the same earthquake acceleration as that for Test No.4. A total of six PDTs were conducted before the final cyclic loading test. After the pseudo dynamic tests, all the BRBs were not damaged. Therefore, cyclic increasing story drifts were imposed until the failure of the BRBs. Since the scheduled PDT and cyclic tests were completed with failures only in bracing components including the BRBs, UBs and the gusset plates, it was decided that Phase-2 tests be conducted after repairing the damaged components. Due to the buckling to the gusset plates observed in the brace-to-column joints in the Phase-1 tests, additional stiffeners were added at the free edges of the gusset at the two third floor brace-to-column joints after the buckled gussets were heat straightened. In addition, the laterally buckled gusset plate under the 3rd floor beam was removed before installing a new one. Six new BRBs, two all metal double cored construction for the 1st story, four concrete filled double cored for the 2nd and 3rd stories, have been installed. Phase-2 tests not only allowed to make the best use of the 3-story, 3-bay frame but also aimed to investigate the performance of the stiffened gussets plates and the new BRBs. The ground motion accelerations applied in Phase 2 PDTs are also shown in Fig. 2. Details of the observation and discussion for the PDTs are summarized in the reference papers (Tsai et al., 2004; Chen et al., 2004; Lin et al., 2004).

BEHAVIOR OF GUSSET PLATES

As mentioned above, at the beginning of Test No.1 in Phase 1, the gusset at first story buckled out of plane as shown in Fig.4(a). The test was stopped for inspection, followed by adding stiffeners shown in Fig. 3 to the edges of the gussets (only to the ones under the beam bottom flange) from 1st story to 3rd story. The situations before and after adding stiffeners are shown in Fig. 4. Stress in the gusset plate is very complex when external load is acting on it, thus some simplified design methods proposed by Whitmore (1952) have been adopted for the design of the gussets. Whitmore suggested that the location of the peak stress can be defined in a “Whitmore Section” where the stresses distributed along a 30 degree angle from the line connecting the first bolt hole to the last bolt hole (Fig. 5). The section within the extended width is called the “Whitmore Section”, and the greatest stress would occur within this section. When the tensile stress on Whitmore Section reaches the yield stress of the gusset Fy, the corresponding brace force defines the tensile capacity of the gusset plate. When the gusset plate is under compression, compressive stress on Whitmore Section may not be able to develop Fy. To prevent the gusset plate from buckling, buckling strength should be checked against the design compressive load. Thornton further suggested (Thornton, 1984) that from the midpoint or the two ends of the Whitmore Width along the force direction to the beam or column flanges, the longest length, L_c of three lines L_1, L_2, and L_3 as shown in Fig. 5 can be used to as the most critical effective length. An effective length factor K of 0.65 has been suggested by Thornton. Thus, capacity design criteria of gusset under tension and compression conditions are summarized in equation (1) and (2).

$$P_{y\ Gusset} = F_y b_e t \geq P_{y\ Brace} \quad for\ \ tension \tag{1}$$

$$P_{cr} = \frac{\pi^2 E}{(KL_c / r)^2}\ b_e\ \ t \geq P_{\max} \quad for\ \ compression \tag{2}$$

By examining the failure modes of the gusset plate shown in Figs. 5 and 6, it appears that the buckling shape at the brace-to-gusset joint in the specimen is similar to that shown in Fig. 6(c). Therefore, before the edge stiffeners were added, the effective length factor might be appropriate to assume it is about 2.0, instead of 0.65. The results of the calculations are shown in Table 2. It's evident that the critical loads P_{cr} of the gussets become quite small when the effective factor, K is 2.0. The critical load P_{cr}, using K=2.0 for the top gusset plate at the first story BRB is about 842kN, closely agree with the experimental buckling load (805*kN*) observed. After adding the edge stiffeners at this gusset and repairing the BRB, the gusset plate (having an effective length factor of 0.65) sustained the rest of all tests. For the bottom gusset at the third story, the critical load of the gusset plate (without the edge stiffeners, assuming K=2.0) is also very close to the ultimate compressive load P_{max} of the third story BRB. This could be used to explain why the gussets at bottom end of BRBs in 3rd story buckled during the subsequent cyclic loads in the Phase I tests. Further, after stiffening the gussets, there was no more gussets buckling occurred in the Phase II tests. It appears that after adding edge stiffeners, the boundary condition is closer to that shown in Fig. 6(d). Thus, it is suggested that the effective length factor can be assumed as 0.65 for the capacity design of the gusset only when the gusset plate is stiffened properly.

Finite Element Analysis using ABAQUS was further conducted to check the buckling strength of gusset plate. The finite element material model for the gusset plate is the bi-linear strain-hardening using the actual material coupon strength. The FE meshes are shown in Fig. 7(a). For the un-stiffen gusset, the FE buckling load is equal to 0.43P_{max}(=750kN) which is close to the experimental buckling load (805kN). After adding stiffeners to the gusset as shown in Fig. 7(b), the buckling load of the gusset is increasing to 3.49P_{max}. Evidently, the out-of-plane buckling has been prevented.

GUSSET ASSESSMENT OF A 2-STORY BRB STEEL FRAME SPECIMEN

In order to further investigate the seismic performance of the BRBF and the gusset connections subjected to the bi-directional earthquake loads, a full-scale 2-story single-bay BRBF specimen has been constructed for substructure pseudo-dynamic testing at NCREE. Because of the pre-mature buckling of the gusset plate in the 3-story CFT/BRB specimen, the gusset plates are properly stiffened using the criteria noted above. For all the gusset plates, extensive ABAQUS finite element analyses have been used to verify the buckling strength of the final designs. Before finalizing the size and location of the stiffeners, ABAQUS finite element analyses were also performed to examine the effectiveness of various stiffening schemes for the gusset plate. The 2-story BRBF substructure shown in Fig. 8 is employed in this experimental research. The prototype two-story building consists of 4-bay by 3-bay. Beam-to-column joints at the perimeter frame are all moment connection, and all other joints in gravity floor framing and braced frames are pin connection. A double-core BRB has been installed in each floor. All beams and columns are wide flange section. The frame are scheduled to be tested in the end of March 2005 using the pseudo-dynamic test procedures applying input ground motions scaled to represent, 50%, 10% and 2% in 50 years seismic hazard levels (Weng et al. 2005). Axial gravity load in the column is simulated by using vertical post-tension steel bars. The bottom end of the post-tensioned steel bars is anchored to the strong floor using a two-directional hinge, and the top end is attached to a cross-beam above the column top. It is assumed that each column is subjected to 70 tons (686 kN) of gravity load from each floor, thus, a total of 140 tons (1372 kN) axial force will be applied on each column.

The final gusset plate designs are shown in Fig. 9. The gusset plates of the 2-story BRBF are designed using Uniform Force Method (AISC, 1998) and method proposed by Whitmore and Thornton noted above. Three possible locations of adding stiffeners are shown in Fig. 10. Stiffener1 is the longer free edge stiffener, Stiffener3 is the shorter free edge stiffener, and Stiffener 2 is along the centerline of the BRB. The dimensions of stiffeners are shown in Table 3. The finite element material model for steel is the bi-linear strain-hardening. The nominal strength for A572 Gr.50 (F_y=352MPa, F_u=458MPa) is assumed. The mesh of C3D20 solid elements is shown in Fig. 11, and the gusset plate is assumed fixed (Fig. 12) at edges along the beam and column flanges in order to simulate the welding between gusset plate and the connecting members. Similar to the ABAQUS analysis noted above, "Eigenvalue Bucking Prediction" procedures were adopted by applying the maximum BRB compression force P_{max} at the brace end. The resulting eigenvalues are tabulated in Table.4. The listed values suggest the buckling strength of the gusset plates normalized with respect to the applied load P_{max}. If the listed eigenvalue is less than one, it implies that the stiffener must be added to resist the P_{max} without buckling. For example, the listed value of 0.8 for the un-stiffened Gusset 2 is not acceptable and the Stiffeners 1 and 3 (with a strength factor of 4.74) enhance the buckling capacity cost effectively. Without any stiffeners, Gusset 4 already has a strength factor of 3.10, it is judged that no stiffener is required there. The final fabrications of the four gusset joints are given in Fig. 13. Networked pseudo dynamic test results can be viewed from the web site (http://substructure-brbf.ncree.org).

SUMMARY AND CONCLUSIONS

Based on these analyses, summary and conclusions are made as follows:

1. Stiffeners added along the free edges of the gusset plate are effective in preventing out-of-plane instability of the brace-to-column connections.
2. When the gusset is not properly stiffened, the effective length factor K should be 2.0 instead of 0.65 when using the buckling criteria proposed by Whitmore and Thornton.
3. Based on the finite element analysis of the 2-story BRBF specimen, the final stiffening schemes have been selected. For Gussets 1 and Gusset 3, Stiffener Type 3 is used. For Gusset 2, both Stiffener Type 2 and 3 are used. Gusset 4 can develop the peak BRB force without adding any stiffener, thus no stiffener is added for Gusset 4. All the stiffeners are welded to both the gusset and the beam flange.
4. It is important to note that the added stiffeners also increase the rotational stiffness of the brace to gusset joint. Thus, it also increases the flexural demand on the buckling restrained braces. Further research on the brace-to-gusset connection details is warranted.

REFERENCES

AISC (American Institute of Steel Construction) (1999). *Manual of Steel Construction: Load & Resistance Factor Design Volume II Connections,* Chicago, IL.

Chen, C.H., Hsiao, P.C., Lai, J.W., Lin, M.L., Weng, Y.T., and Tsai K.C. (2004). "Pseudo-Dynamic Test of a Full-Scale CFT/BRB Frame: Part 2 - Construction and Testing." *Proceedings of 13th World Conference on Earthquake Engineering,* Vancouver, B.C., Canada, Paper No. 2175.

Lin, M.L., Weng, Y.T., Tsai, K.C., Hsiao, P.C., Chen, C.H. and Lai, J.W. (2004). "Pseudo-Dynamic Test of a Full-Scale CFT/BRB Frame: Part 3 - Analysis and Performance Evaluation." *Proceedings of 13th World Conference on Earthquake Engineering,* Vancouver, Canada. Paper No. 2173.

Tsai, K.C., Weng, Y.T., Lin, S.L., and Goel, subhash. (2004). "Pseudo-Dynamic Test of a Full-Scale CFT/BRB Frame: Part 1 - Performance Based Specimen Design." *Proceedings of 13th World Conference on Earthquake Engineering,* Vancouver, B.C., Canada, Paper No. 750.

Tsai, K.C., Hwang, Y.C., Weng, C.S, Shirai, T, and Nakamura, H. (2002). "Experimental Tests of Large Scale Buckling Restrained Braces and Frames." *Proceedings, Passive Control Symposium 2002*, Tokyo Institute of Technology, Tokyo.

Tsai, K.C. and Lin, S.L. (2003a). *Study of All Metal and Detachable Buckling Restrained Braces*, Center for Earthquake Engineering Research, National Taiwan University, Report No. CEER/R92-08.

Tsai, K.C., and Lin, B.C (2003b). *User Manual for the Platform and Visualization of Inelastic Structural Analysis of 2D Systems PISA3D and VISA3D*, Center for Earthquake Engineering Research, National Taiwan University, Report No. CEER/R92-07.

Thornton, W.A. (1984). "Bracing Connections for Heavy Construction." *Engineering Journal of AISC,* Vol.21, No.3, pp. 139~148.

Uang, C.M., Nakashima, M. and Tsai, K.C. (2004). "Research and Applications of Buckling Restrained Braced Frames." *International Journal of Steel Structures*, 4/2004.

Whitmore, R.E. (1952). *Experimental Investigation of Stresses in Gusset Plates*, Bulletin No.16, Engineering Experiment Station, University of Tennessee.

Weng, Y. T., Lin, J. L., Tsai, C. Y., and Tsai, K. C. (2005). "Analytical assessment of a 2-story BRBF for full-scale 3D sub-structural pseudo-dynamic testing." *The First Conference on Advanced in Experimental Structural Engineering (AESE)*, Nagoya, Japan.

Table 1 Selection of member sizes and grades

Member	Beam Sizes and Core Cross Sectional Area of Braces (A572 GR50)		
Location	1FL	2FL	3FL
Beam (mm)	H456×201×10×17	H450×200×9×14	H400×200×8×13
Brace (cm^2)	30	25	15
Dimension of Columns (A572 GR50) unit : mm	CFTs: C1: Tube: 350×9, C2: Pipe: 400×400×9		

Table 2 Capacity check of gusset plates

		Gusset Plate (kN)			BRB (kN)	
		$P_{y\ Gusset}$	P_{cr} (K=2.0)	P_{cr} (K=0.65)	$P_{y\ Brace}$	P_{max}
1F	Top	2287	842	7975	1558	1713
	Bottom	2287	1367	12939	1558	1713
3F	Top	1397	603	5709	686	755
	Bottom	1397	743	7036	686	755

Table 3 Dimension of stiffeners

Gusset	Stiffener Plate (mm)	
	No.	Dimension
Gusset 1	1	150x810x10
	2	50x242x10
	3	180x300x12
Gusset 2	1	150x1120x10
	2	70x575x10
	3	330x300x12
Gusset 3	1	150x770x10
	2	70x240x10
	3	116x300x12

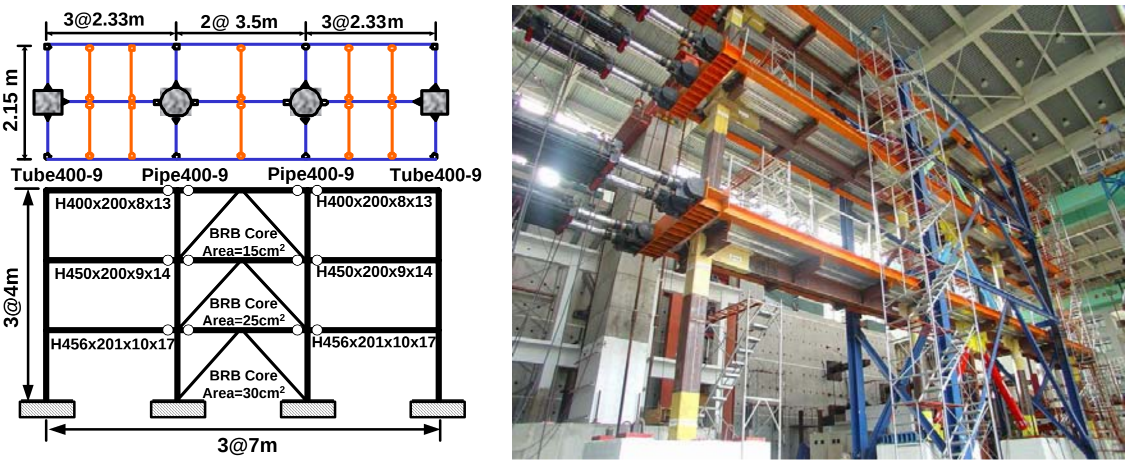

(a) (b)

Fig. 1 (a) Plan and elevation of the full-scale CFT/BRB composite frame
(b) Photo of the CFT/BRB frame specimen

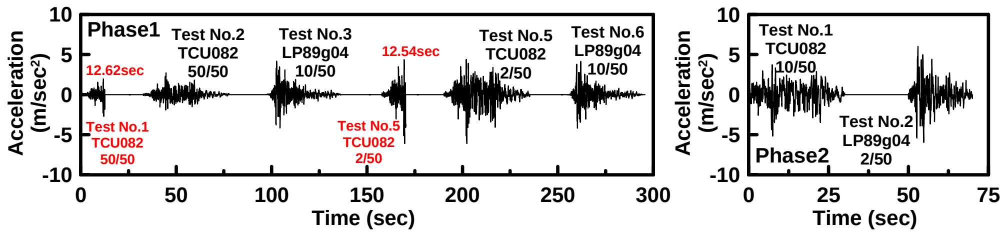

Fig. 2 Ground acceleration time history in PDTs

Table 4 Effect of adding various stiffeners in four gusset plates

Gusset	Stiffener Plate	Eigenvalue (1^{st} mode)
Gusset 1 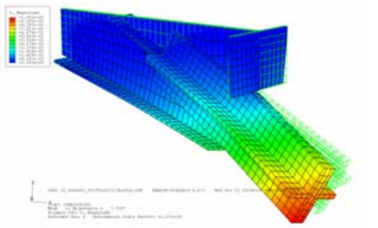	Un-stiffen	2.45
	1	2.64
	2	2.52
	3 (used)	**7.41**
	1&2	2.72
	1&3	2.76
	2&3	7.44
	1&2&3	7.77
Gusset 2 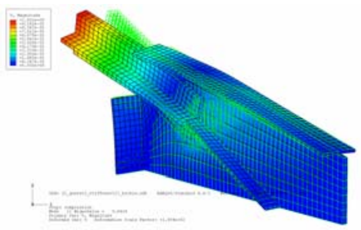	Un-stiffen	0.8
	1	1.06
	2	1.04
	3	3.93
	1&2	1.30
	1&3	5.46
	2&3 (used)	**4.74**
	1&2&3	5.84
Gusset 3 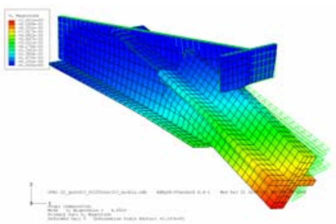	Un-stiffen	1.83
	1	2.04
	2	1.99
	3 (used)	**4.30**
	1&2	2.24
	1&3	4.56
	2&3	4.83
	1&2&3	4.65
Gusset 4 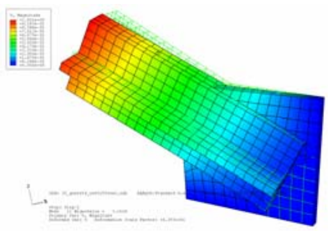	**Un-stiffen (used)**	**3.10**

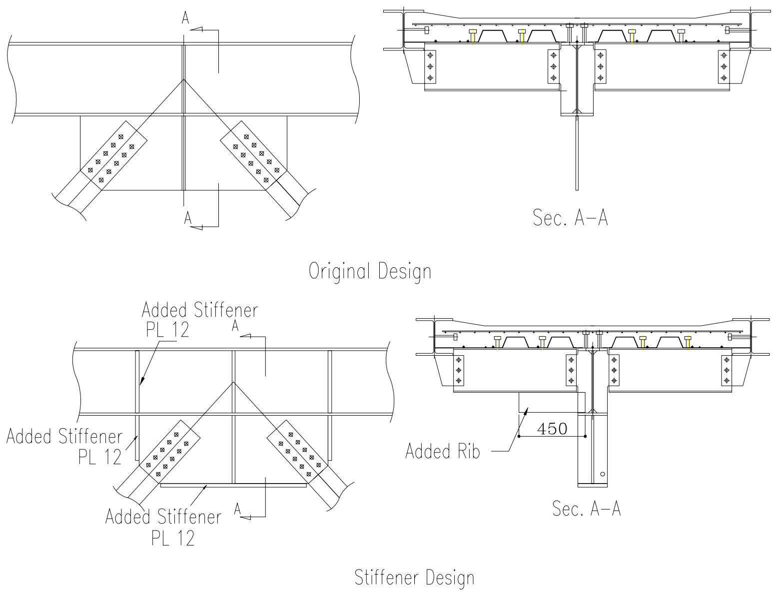

Fig. 3 (a) Original design of the gusset plate and (b) Details of added stiffeners

Fig. 4. (a) Out-of-plane buckling of the gusset plate (b) Gusset plate after adding stiffeners

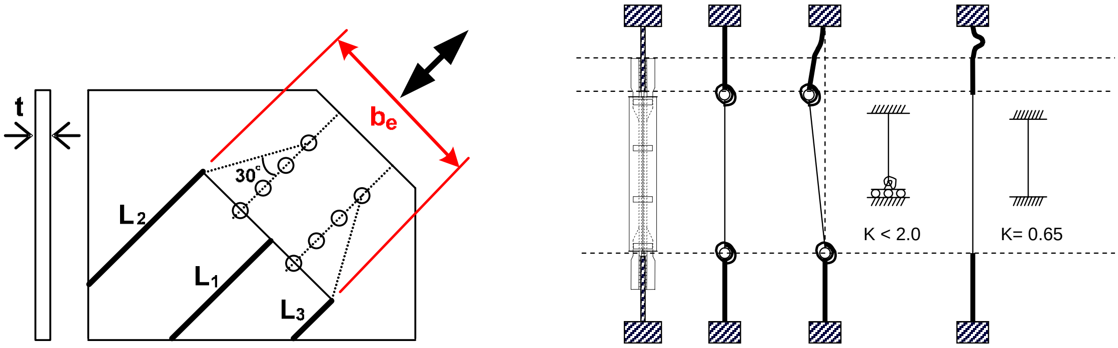

Fig. 5 Whitmore's and Thornton's design methodologies

(a) (b) (c) (d)

Fig. 6 Brace boundary conditions and buckling modes

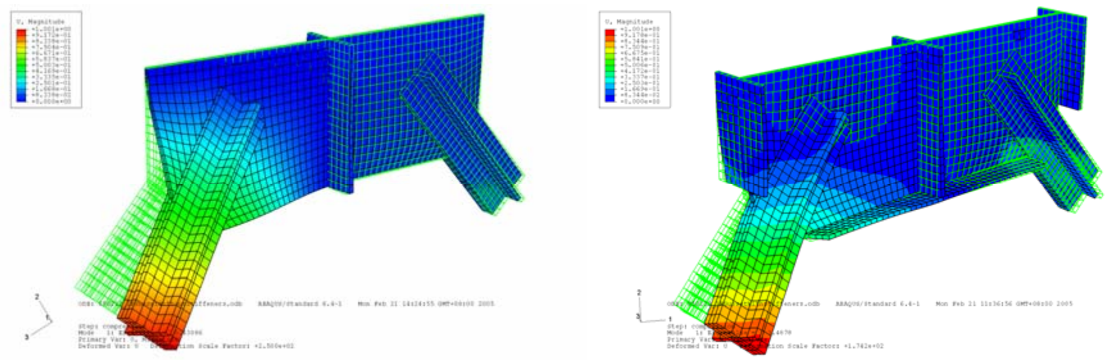

Fig. 7 (a) FE Model of un-stiffened gusset plate (b) FE Model of stiffened gusset plate

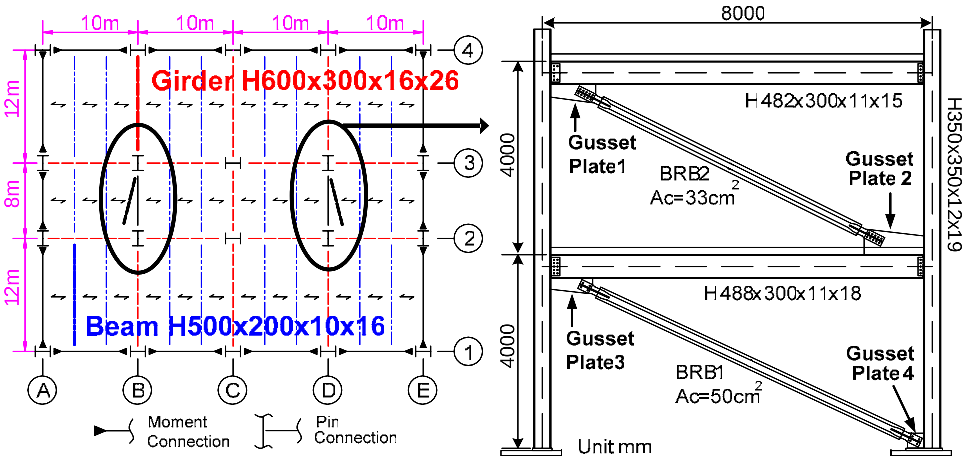

Fig. 8 Floor framing plan and BRBF elevation

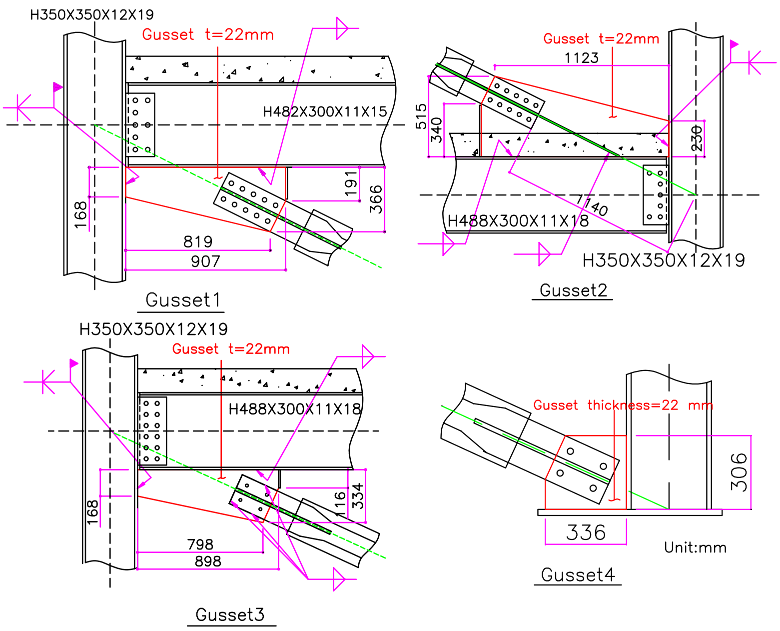

Fig. 9 Details at the gusset plate connections

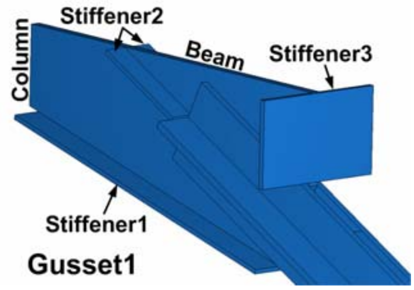

Fig. 10 Three possible locations of adding stiffeners for the gusset plate

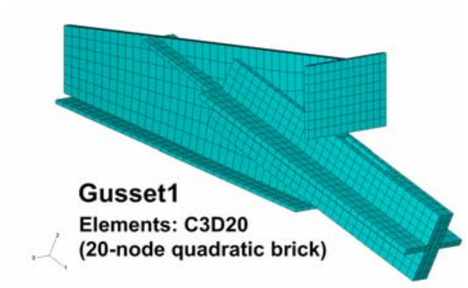

Fig. 11 Finite element mesh of Gusset 1

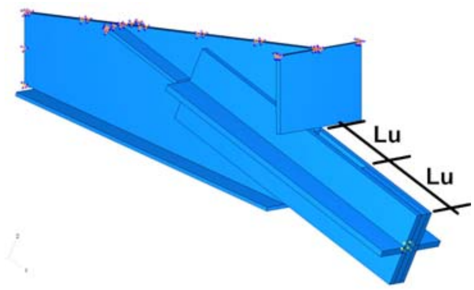

Fig. 12 Boundary condition of the Gusset 1

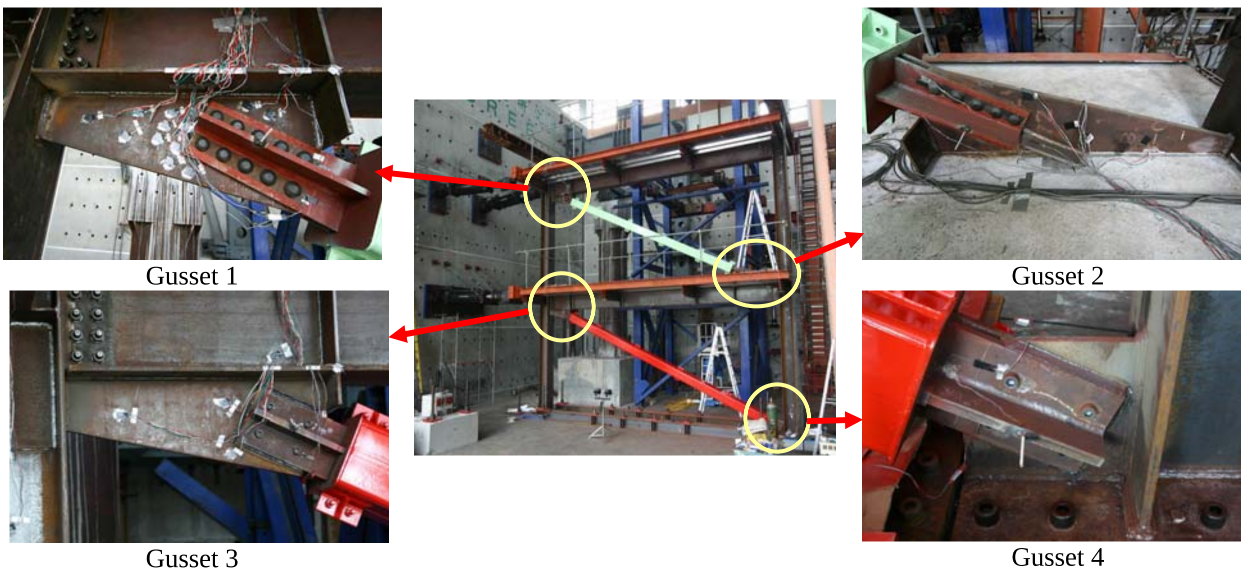

Fig. 13 Final fabrications of the four gusset plates